THE JOURNAL OF PHYSICAL CHEMISTRY A

Article

pubs.acs.org/JPCA

Dressed Adiabatic and Diabatic Potentials for the Renner−Teller/Jahn−Teller F + H_2 System

A. Csehi,[†] A. Bende,[‡] G. J. Halász,[†] Á. Vibók,[§] A. Das,[∥] D. Mukhopadhyay,[∥] S. Mukherjee,[⊥] S. Adhikari,[⊥] and Michael Baer*[,⊥]

[†]Department of Information Technology, University of Debrecen, P.O. Box 12, H-4010 Debrecen, Hungary

[‡]Molecular and Biomolecular Physics Department, National Institute for Research and Development of Isotopic and Molecular Technologies, Cluj-Napoca, Romania

[§]Department of Theoretical Physics, University of Debrecen, P.O. Box 5, H-4010 Debrecen, Hungary

[∥]Department of Chemistry, University of Calcutta, Kolkata 700 009, India

[⊥]Department of Physical Chemistry, Indian Association for Cultivation of Science, Jadavpur, Kolkata 700 032, India

[#]The Fritz Haber Research Center for Molecular Dynamics, The Hebrew University of Jerusalem, Jerusalem 91904, Israel

ABSTRACT: We follow a suggestion by Lipoff and Herschbach (*Mol. Phys.* **2010**, *108*, 1133) and compare *dressed* potentials to get insight regarding the low-energy dynamics (e.g., *cold reaction*) taking place in molecular systems. In this particular case we are interested in studying the effect of topological effects on the interacting atoms. For this purpose we consider dressed *adiabatic* and adiabatic-via-dressed *diabatic* potentials in the entrance channel of reactive systems. In a recent study of this kind for the F + H_2 system (*J. Chem. Phys.* **2012**, *136*, 054104), we revealed that a single Jahn−Teller conical intersection is expected to have only a mild effect on the dynamics. This fact implies that the Born−Oppenheimer approximation is expected to be valid for this system at least for low enough energies. In the present article this study is extended to include also the Renner-Teller effect as produced by the two lower degenerate Π states. As a result we consider three electronic states which enforce the use of the adiabatic-to-diabatic transformation (ADT) matrix A. The results indicate that the topological effects as produced by the extended Renner/Teller-Jahn/Teller system are strong to the level that, most likely, abolishes the Born−Oppenheimer approximation for this system, all this in contrast to our previous findings (see above publication).

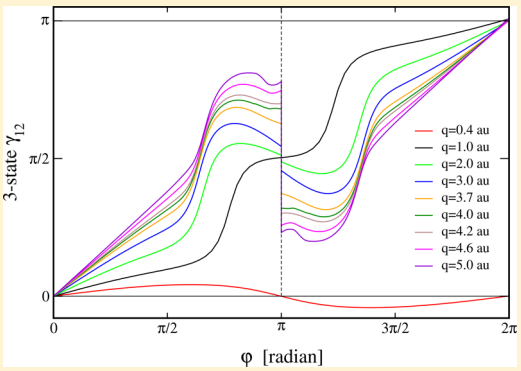

I. INTRODUCTION

In this article we continue with our efforts to form reliable rigorous, single-valued diabatic potential energy surfaces (PES). In recent articles on this issue it was suggested to apply an approach based on *complementary* line integrals.[1] Although this approach fulfilled part of the above expectations, it has one significant drawback, namely, it is *approximate*. In this article we hope to overcome this shortcoming and present an approach that is more accurate although, eventually, subject to convergence processes.

Diabatic PESs, for this system have existed for numerous years. However, their main deficiency is that instead of using mixing angles based on Born−Oppenheimer (BO) ingredients they were calculated by analyzing the coefficients in the configuration interaction expansion of the FH_2 wave function.[2]

In the present article we consider an advanced approach that is expected to yield more accurate diabatic PESs.[3] It is based on a group of three interacting states that contain two Π states and one Σ state. Here the two Π states, of symmetries 1A′ and 1A″, form the Renner−Teller (RT) degeneracy line along the collinear axis of the relevant molecule and the two states of symmetry 1A′ and 2A′ (where the first is the just mentioned Π state and the second a Σ state) form a quasi-Jahn−Teller (JT) degeneracy at a *point on this axis*.[2a] This situation leads to a new topological effect that was termed by us as the RT/JT effect.[3]

The resulting effect of the two types of interaction is treated via a matrix that contains the relevant nonadiabatic coupling terms (NACT)[4,5] which, in the present case, will be of dimension 3 × 3. Having the NACT matrix we proceed by calculating the corresponding adiabatic-to-diabatic transformation (ADT) matrix, which finally yields the required diabatic potential energy surfaces (PES).

Because our aim is to derive diabatic PESs, we have to guarantee that the approach to be developed yields ADT matrices based reliably on the two kinds of NACTs. In previous studies[6,7] this was achieved by employing line integrals along

Special Issue: Structure and Dynamics: ESDMC, IACS-2013

Received: November 7, 2012
Revised: December 20, 2012
Published: December 20, 2012

contours that *surround* the *collinear* axis, where the NACTs matrices contained both the RT and the JT NACTs.

The main shortcoming of this approach is that the ADT matrices are calculated for grids on a series of planes perpendicular to the collinear axis. However, because our aim is to calculate PESs for the full chemical volume we need the ADT matrices to be derived for grids on *triatomic* planes. (We remind the reader that the *dynamical treatments* are carried out on triatomic planes.) In other words, the just mentioned approach demands complicated transformations from these perpendicular grids to the triatomic grid—a process that may cause severe difficulties to the dynamical treatment. In what follows we suggest calculating the ADT matrices *directly* for the triatomic planar grid. Another good reason for doing it this way is that, for each value of the vibrational coordinate r, such a plane contains *all* JT conical-intersections (*ci*) as well as the collinear axis that contains *all* RT degeneracy points.

However, there is still one hurdle to overcome. Because all contours are assumed to be in the plane, no contour is capable of surrounding this axis (which is in the plane) and, therefore, a different way to include the RT effect has to be found. On the basis of our past experience[8,9] a reliable way to include the RT effect is to let the contours intersect the degeneracy line and in this way to enable the NACT matrix elements to pick up this effect. The only problem encountered here is that these calculated NACTs are extremely spiky, reminiscent of the Dirac δ-function (see, e.g., Figure 2 in ref 9a), and therefore their correct *normalization* can be missed.

This situation opened up the way for a theoretical study which showed that these NACTs are indeed, up to a normalization factor, pure Dirac δ-functions.[9b,18a] The theoretical findings of this study are incorporated in the present study (see eqs 7).

In this article we report on the first diabatic potentials, based on this new type of RT/JT NACTs, presented as *planar* equipotential lines for the HHF system. The planes are parametrized via values of r (the interatomic distance of H_2) and formed by an (R, θ) grid where R and θ are the polar coordinates of the fluorine with respect to the center-of-mass of the H_2 molecule (Figure 1).[1] The dimensions of the planar configuration spaces (CS) are $2.9 < R < 10$ au and $-\pi/2 < \theta < +\pi/2$.

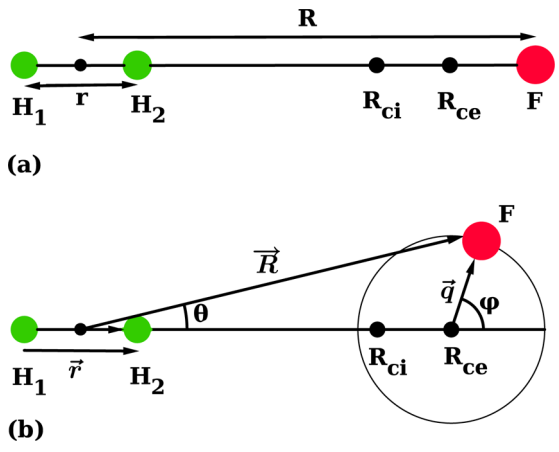

Figure 1. System of coordinates: (a) positions of atoms, point of (1,2) *ci* and the center of all circular contours. (b) System of coordinates: $(R, \theta|r)$ vs $(\varphi, q|r)$.

Our main goal is to present the just mentioned RT/JT PESs but there is another reason for this study, namely, to find out to what extent the topological features of this system may affect the Born–Oppenheimer (BO) approximation for this system. To clarify what we have in mind, we refer to a recent article by Lipoff and Herschbach (LH)[10] in which they distinguish between *bare* and *dressed* potentials (while referring to the reactive F + H_2 system). Following this presentation, the *bare* PES is the one obtained from the electronic structure calculations (in other words, the BO lowest adiabatic PES) and the *dressed* PES is the effective potential felt by the reactants while approaching each other at (very) low temperatures (as encountered, e.g., in *cold reactions*[11]). Following this study LH concluded (just like Rosenman et al. a few years earlier[12]) that the dressed potential contains important physical information concerning the low energy dynamics.

This idea was adopted by us in our recent publication,[1a] with a certain twist. We are not really interested in the bare potential but in the comparison between two types of *dressed* adiabatic potentials: the ordinary one as formed by the lowest BO *adiabatic* PES and the second as formed by the two lowest dressed *diabatic* potentials (see ref 1a, as well as section II.5, for details) and which therefore contains the relevant topological effects. In that study, which was based on *complementary* line integrals, we hardly encountered any effect of the topological features on the lowest adiabatic PES, thus concluding that topological effects are not expected in this system. A similar study is carried out in the present article for the RT/JT effects but, as will be seen, with different consequences.

Although the theory based on this new type of NACTs is presented, in detail, elsewhere,[3] we briefly elaborate on it again for the sake of completeness.

The article is arranged in the following way: In section II is given the theoretical background, which concentrates on the NACT matrices, on the corresponding extended (privileged) two-state ADT (mixing) angles and finally referring to the derivation of the Renner–Jahn parameter η, in section III are presented the calculations and in section IV is given the discussion and summary of the results.

Finally, we make the following comment: In the present study, just like in our recent studies,[1] we do not include the spin–orbit (SO) coupling (such calculations were reported, e.g., in refs 2b and 2c). It is very likely that as long as this coupling is ignored, the corresponding *dynamic* calculations are not complete, but our main concern, at this stage, is the BO adiabatic and diabatic potentials and not the actual dynamic calculations.

II. THEORETICAL BACKGROUND

II.1. Introductory Remarks. Our approach is based on solving the following multidimensional first-order differential equation[4,5]

$$\nabla \mathbf{A}(\mathbf{s}) + \boldsymbol{\tau}(\mathbf{s})\,\mathbf{A}(\mathbf{s}) = 0 \qquad (1)$$

where $\mathbf{A}(\mathbf{s})$, as previously mentioned, is the ADT matrix, $\boldsymbol{\tau}(\mathbf{s})$ is an antisymmetric matrix that contains the above-mentioned vectorial NACTs, and $\mathbf{s}$ is a variable that presents the collection of internal nuclear coordinates. The matrix $\boldsymbol{\tau}(\mathbf{s})$, which frequently contains *singular* elements, appears (together with the *adiabatic*, diagonal PES, $\mathbf{u}(\mathbf{s})$) in the nuclear Schrödinger equation (SE) following the Born–Oppenheimer (BO) treatment.[13] One way to avoid these *singularities* is to eliminate

dx.doi.org/10.1021/jp311014z | J. Phys. Chem. A 2013, 117, 8497–8505

the $\boldsymbol{\tau}(\mathbf{s})$ matrix and form a modified SE free of all singularities but governed by $\mathbf{V}(\mathbf{s})$, a *full* potential matrix, which replaces the original, *diagonal* matrix, $\mathbf{u}(\mathbf{s})$. The two potential matrices are related via the following transformation:[4,5]

$$\mathbf{V}(\mathbf{s}) = \mathbf{A}(\mathbf{s})^{\dagger}\, \mathbf{u}(\mathbf{s})\, \mathbf{A}(\mathbf{s}) \tag{2}$$

where $\mathbf{A}(\mathbf{s})^{\dagger}$ is the complex conjugate matrix of $\mathbf{A}(\mathbf{s})$. The matrix $\mathbf{V}(\mathbf{s})$ is known as the *diabatic* PES—its diagonal elements are the corresponding diabatic potentials and its off-diagonal elements form the diabatic *coupling* terms (reminiscent of the NACTs).

The common way to solve eq 1 is to assume contours, Γ, and to integrate it along such contours. Because $\mathbf{V}(\mathbf{s})$ has to be presented at a given grid of points, we must guarantee that the chosen contours (along which $\mathbf{A}(\mathbf{s})$ and $\mathbf{V}(\mathbf{s})$, are calculated) *cover* efficiently the full corresponding CS. While doing that, we face again the troublesome singularities of the matrix $\boldsymbol{\tau}(\mathbf{s})$, which are also known as points of *conical/parabolical intersections*.[14] These *intersections* may cause the diabatic potential $\mathbf{V}(\mathbf{s})$ to be multivalued (namely, non-single-valued) and, therefore, essentially, of no physical use. To overcome this difficulty, the $\mathbf{A}$ matrix (which, according to eq 2, is responsible for the single-valuedness of $\mathbf{V}(\mathbf{s})$) has to be calculated by employing numerous (usually 3−4) states so that upon completion of any closed contour in that CS it ends up as a *diagonal* matrix.[15]

An efficient way to treat these matrices is as follows: Because $\mathbf{A}(\mathbf{s})$ is an *orthogonal* matrix, it can be presented in terms of Euler-type angles[7,16] and consequently its *diagonality* at the end of a closed contour is guaranteed if and only if these angles, become *integer* multiples of π.

II.2. Nonadiabatic Coupling Transformation Matrix. Next our aim is to construct NACT matrices, $\boldsymbol{\tau}(\mathbf{s})$, which contain the two types of NACTs: the quasi-JT NACTs and the RT NACTs. This is done for a system of three states, two A′ and one A″.[3b] Here the coupling between 1A′ and 2A′ is of the quasi-JT-type and is designated as $\boldsymbol{\tau}_{12}$ and the coupling between 1A′ and 1A″ is of the RT-type and is designated as $\boldsymbol{\tau}_{11''}$ (see Figure 2 in ref 3b). We remind the reader that the two states 1A′and 1A″ form a RT degeneracy line along the collinear HHF axis.

The NACT-matrix takes the form

$$\boldsymbol{\tau}(\mathbf{s}) = \begin{pmatrix} 0 & \tau_{11''} & \tau_{12} \\ -\tau_{11''} & 0 & 0 \\ -\tau_{12} & 0 & 0 \end{pmatrix} \tag{3}$$

where we assumed that $\tau_{21''} \equiv 0$.

However, this form is not convenient for numerical treatment as we prefer to have τ_{12} at the (1,2) position of $\boldsymbol{\tau}(\mathbf{s})$. To achieve this arrangement, we permute between the last two rows and then between the last two columns so that $\boldsymbol{\tau}(\mathbf{s})$ becomes

$$\boldsymbol{\tau}(\mathbf{s}) = \begin{pmatrix} 0 & \tau_{12} & \tau_{11''} \\ -\tau_{12} & 0 & 0 \\ -\tau_{11''} & 0 & 0 \end{pmatrix} \tag{3′}$$

which is the NACT matrix of the desired form. It is important to mention that the solution of eq 1 is not affected by these permutations.

II.3. Adiabatic-to-Diabatic Transformation Matrix and Privileged Angle. In the early days we used to solve eq 1 by treating the full $\mathbf{A}$ matrix as it stands without paying much attention to its internal structure. The only exceptional case is the two-state case where the $\mathbf{A}$ matrix which can be expressed in terms of one angle $\gamma(\mathbf{s})$ (to be termed as the ADT or mixing angle) and this leads to the following simple line *integral*: $\gamma_{12}(\mathbf{s}|\Gamma) = \int_{\mathbf{s}_0}^{\mathbf{s}} d\mathbf{s}'\cdot\boldsymbol{\tau}_{12}(\mathbf{s}'|\Gamma)$.[4] Here $\tau_{12}(\mathbf{s}|\Gamma)$ is the (1,2) NACT matrix element, Γ designates the contour along which is carried out the integration and the dot presents the scalar product. Because we intend to consider circular contours $\tau_{12}(\mathbf{s}|\Gamma)$ is replaced by $(1/q)\boldsymbol{\tau}_{\varphi 12}(\varphi,q)$, so that the integration becomes over an angle, φ:

$$\gamma_{12}(\varphi,q) = \int_0^{\varphi} \boldsymbol{\tau}_{\varphi 12}(\varphi',q)\, d\varphi' \tag{4}$$

where (φ, q) are polar coordinates: q is the radius and φ is the angle associated with the (nuclear) rotation. For completeness we mention that $\boldsymbol{\tau}_{\varphi 12}(\varphi,q)$ is defined as

$$\boldsymbol{\tau}_{\varphi 12}(\varphi,q) = \langle \zeta_1(\mathbf{s}_e|\varphi,q)|\frac{\partial}{\partial\varphi}\zeta_2(\mathbf{s}_e|\varphi,q)\rangle$$

Here $\zeta_j(\mathbf{s}_e|\varphi,q)$, j = 1, 2, are the corresponding eigenfunctions related to the two states under consideration. In addition to the ADT angle we are also interested in the angle $\alpha_{12}(q)$—*the-end-of-the-contour phase*—defined as[15]

$$\alpha_{12}(q) = \int_0^{2\pi} \boldsymbol{\tau}_{\varphi 12}(\varphi',q)\, d\varphi' \tag{5}$$

α_{12} is known as the *topological/geometrical* phase.

To treat a tristate system (as encountered here), we take advantage of the fact that the 3 × 3 $\mathbf{A}(\varphi,q)$ matrix is an orthogonal matrix and, therefore, its nine elements can be presented in terms of the three quasi-Euler angles.[16] As in the case of the ordinary Euler matrix, the orthogonal $\mathbf{A}$ matrix is presented as a product of *three rotation* matrices $\mathbf{Q}_{ij}(\gamma_{ij})$ $(i < j = 2, 3)$ where the product $\mathbf{A} = \mathbf{Q}_{kl}\mathbf{Q}_{mn}\mathbf{Q}_{pq}$ can be written in any order. Substituting this product in eq 1 yields three coupled first-order differential equations for the three corresponding quasi-Euler angles, γ_{ij}. The final set of equations as well as their solution depends on the order of the $\mathbf{Q}$ matrices.[16b]

In an analysis carried out several years ago[7a,17] we attributed physical meaning only to one of the three ADT angles, γ_{ij}, privileged with an equation that contains the corresponding NACT, τ_{ij}, as a free *isolated* term (there is one such equation in every group of three coupled equations). In what follows we assume γ_{12} to be such an angle and consider for this purpose the product: $\mathbf{A} = \mathbf{Q}_{12}(\gamma_{12})\,\mathbf{Q}_{13}(\gamma_{13})\,\mathbf{Q}_{23}(\gamma_{23})$. Substituting this product in eq 1 yields three first-order equations, of which two equations (for γ_{12} and γ_{13}) form a closed subgroup of two coupled equations:[3a,7a]

$$\frac{\partial}{\partial\varphi}\gamma_{12} = -\tau_{12} - \tan\gamma_{13}(\tau_{23}\cos\gamma_{12} + \tau_{13}\sin\gamma_{12}) \tag{6a}$$

$$\frac{\partial}{\partial\varphi}\gamma_{13} = \tau_{23}\sin\gamma_{12} - \tau_{13}\cos\gamma_{12} \tag{6b}$$

These two equations are solved with the aim of calculating the privileged ADT angle $\gamma_{12}(\varphi,q)$. The introduction of the *privileged* angle enables the extension of the earlier defined two-state topological phase, α_{12}, to three-state systems. A

dx.doi.org/10.1021/jp311014z | J. Phys. Chem. A 2013, 117, 8497−8505

straightforward choice for this purpose is the *end-of-the-contour* value of the angle γ_{12}. Thus $\alpha_{12}(q) = \gamma_{12}(\varphi{=}2\pi,q)$.

II.4. Inclusion of the Renner–Teller Effect. *II.4.1. Presentation of the Intraplanar RT NACT.* Whereas the calculations of two-state JT-NACTs along circular contours, Γ, in the triatomic plane is well-known, we concentrate mainly on the RT-NACT, $\tau_{11''}$, along the *same* contour (see section II.2). As already mentioned earlier, we consider circles that have their *centers* on the collinear axis. Because the collinear axis is an infinitely long interval $-\infty < R < +\infty$ each such circle intersects this line at two points, i.e., at $\varphi = 0$ and at $\varphi = \pi$ (see Figure 1b). It is well-known that at *each* such intersection point, along a short interval *perpendicular* to the collinear axis, is formed a spiky nonzero NACT (in this case an angular NACT) with features reminiscent of a Dirac δ-function.[9b,18a] Thus, our first tendency is to assume that the angular RT-NACTs in the planar CS take the form[3]

$$\tau_{11''}(\varphi|q,\Gamma) = \frac{\pi}{2}\delta(\varphi - \vartheta) \tag{7a}$$

for any circle Γ with a radius q (here ϑ designates the intersection points and is either zero or π; see Figure 1b). Equation 7a has to be applied with some care because as it stands it yields, for any circle, a quantized topological phase ($=\pi$) to be expected for an *undisturbed* RT effect along Γ. However, in section II.1 we assumed the existence of a JT *ci* on the *collinear* axis and, therefore, the RT effect is most likely weakened (or, eventually, intensified) by such a *ci*.[18b] Consequently, the pure RT *quantization* is affected and a way to incorporate this fact is to modify eq 7a) by multiplying it with a normalization factor, η (to be determined later; see section II.4.3). Thus

$$\tau_{11''}(\varphi|q,\Gamma) = \frac{\pi}{2}\eta\delta(\varphi - \vartheta) \tag{7b}$$

In what follows, eq 7b is termed as the quasi-Dirac δ-function and η is termed as the Renner–Jahn coupling parameter (RJCP).

Although the circular contour intersects the HHF axis at two points, namely, at $\varphi = 0, \pi$ we consider only what happens at $\varphi = \pi$. It can be shown that the RT-NACT at $\varphi = 0$ has no effect on the results.

II.4.2. RT/JT Coupled Equations. To derive the corresponding differential equations for the tristate RT/JT coupled system we consider the NACT-matrix given in eq 3′ and substitute the relevant matrix elements in eqs 6. Thus

$$\frac{\partial}{\partial\varphi}\gamma_{12}(\varphi) = -\tau_{12}(\varphi) - \tau_{11''}(\varphi)\tan\gamma_{13}(\varphi)\sin\gamma_{12}(\varphi) \tag{8a}$$

$$\frac{\partial}{\partial\varphi}\gamma_{13}(\varphi) = -\tau_{11''}(\varphi)\cos\gamma_{12}(\varphi) \tag{8b}$$

Because the integration is done along circular contours only, the (general) first-order differentiation operator, ∇, is replaced by the angular derivative: $(\partial/\partial\varphi)$. Also, while considering eqs 8 (and similar expressions that follow), we remind the reader that $\gamma_{ij}(\varphi)$ stands for $\gamma_{ij}(\varphi,q)$.

Parts of eqs 8 can be integrated analytically taking advantage of eq 7b. Defining the following Heaviside step-function

$$\Theta(\varphi{-}\pi) = \begin{cases} 0 & 0 \le \varphi \le \pi \\ 1 & \pi \le \varphi \le 2\pi \end{cases} \tag{9}$$

it can be shown that the solution of eq 8b is proportional to this step-function:

$$\gamma_{13}(\varphi) = \Theta(\varphi{-}\pi)\,\gamma_{13}^{(0)}(\varphi) \tag{10a}$$

where

$$\gamma_{13}^{(0)}(\varphi) = -\eta\frac{\pi}{2}\cos\gamma_{12}(\varphi{=}\pi) \tag{10b}$$

and that the solution of eq 8a is also a step-function of a somewhat more involved form

$$\gamma_{12}(\varphi) = \begin{cases} -\int_0^{\varphi} \mathrm{d}\varphi'\ \tau_{12}(\varphi') & 0 \le \varphi \le \pi \\ -\int_0^{\varphi} \mathrm{d}\varphi'\ \tau_{12}(\varphi') + \chi(\varphi{=}\pi) & \pi \le \varphi \le 2\pi \end{cases} \tag{11}$$

where $\chi(\varphi{=}\pi)$ is given in the form

$$\chi(\varphi{=}\pi) = -\eta\frac{\pi}{2}\tan\{\gamma_{13}^{(0)}(\varphi{=}\pi)\}\sin\{\gamma_{12}(\varphi{=}\pi)\} \tag{12}$$

Equation 12 is characterized by the following features: (i) In the case $|\gamma_{12}(\varphi{=}\pi)| > \pi/2$ the sign of $\chi(\varphi{=}\pi)$ is opposite to the sign of $\gamma_{12}(\varphi{=}\pi)$; e.g., when $\gamma_{12}(\varphi{=}\pi) < 0$, then $\chi(\varphi{=}\pi) > 0$. (ii) In the case $|\gamma_{12}(\varphi{=}\pi)| < \pi/2$ the sign of $\chi(\varphi{=}\pi)$ is identical to the sign of $\gamma_{12}(\varphi{=}\pi)$; e.g., when $\gamma_{12}(\varphi{=}\pi) < 0$, then $\chi(\varphi{=}\pi) < 0$.

For the whole approach to be meaningful the upward/downward vertical shifts as given by $\chi(\varphi{=}\pi)$ have to fulfill two conditions:

(1) Because the diabatic potentials have to be single-valued at every point in CS, they have to be *so* also at $\varphi = \pi$. Consequently, the value of $\chi(\varphi{=}\pi)$ has to guarantee the equality: $\sin[\gamma_{12}(\varphi{=}\pi)] = \sin[\gamma_{12}(\varphi{=}\pi){+}\chi]$ and a similar equality (up to a sign) for the cosine function.

(2) Because the value of $\gamma_{12}(\varphi)$ at the end of the closed circular contour, namely, $\gamma_{12}(\varphi{=}2\pi)$ has to be equal to $n\pi$ the vertical shift, $\chi(\varphi{=}\pi)$, has to guarantee the following *quantization* condition:

$$\alpha(q) = -\int_0^{2\pi} \mathrm{d}\varphi'\ \tau_{12}(\varphi') + \chi(\varphi{=}\pi) = n\pi \tag{13}$$

where $\alpha(q)$ is the recognized as the relevant *geometrical* phase (see eq 5)

These conditions will be discussed next, in more detail, for of the case of *small* deviations.

II.4.3. Derivation of the Renner-Jahn coupling parameter η. To derive the RJCP, η, we consider the solution for $\gamma_{12}(\varphi)$ as given in eq 11 for the case that $\gamma_{12}(\varphi{=}\pi)$ is *slightly* larger than $\pi/2$, namely

$$\gamma_{12}(\varphi{=}\pi) = \pi/2 + \varepsilon \tag{14}$$

Here ε is a constant assumed to be *small* enough to guarantee the fulfillment of the required approximations. Substituting eq 14 into eq 12 yields for the corresponding vertical shift, $\chi(\varphi{=}\pi)$, the value[3]

$$\chi(\varphi{=}\pi) = \left(\eta\frac{\pi}{2}\right)^2\varepsilon \tag{15}$$

On the basis of *continuity* we expect that, for $\varepsilon \to 0$, two requirements have to be fulfilled by $\chi(\varphi)$ at $\varphi = \pi$. We start with the single-valuedness, which is fulfilled when $\sin(\pi/2{+}\varepsilon) =$

dx.doi.org/10.1021/jp311014z | J. Phys. Chem. A 2013, 117, 8497–8505

$\sin(\pi/2+\varepsilon-\chi) = \sin(\pi/2-\varepsilon)$ (see Appendix II in ref 3b for additional information). In other words, the single-valuedness is fulfilled when $(\pi/2+\varepsilon-\chi) = (\pi/2-\varepsilon)$ or $\chi = 2\varepsilon$. Recalling eq 15 we see that this happens when η is[3]

$$\eta = \frac{2\sqrt{2}}{\pi} = 0.9003 \tag{16}$$

We continue with the *quantization* requirement and for this purpose we employ eq 13. From eq 14 we get, due to *symmetry*, that $\gamma_{12}(\varphi=2\pi) = \pi + 2\varepsilon$. Substituting this equality in eq 13, we find that the quantization is fulfilled whenever $2\varepsilon - \chi = 0$; thus, as before, this equality yields for η the result given in eq 16.

So far the η value in eq 16 was determined for the case that $\gamma_{12}(\varphi=\pi)$ is *slightly* larger than $\pi/2$ (see eq 14). In ref 3a, we conducted, for the F + H_2 system, a numerical study with the aim of finding out to what extent this value of η applies also for the more common situations. Indeed, for all considered cases (even for vertical shifts up to ~2Rad) we find the differences between the theoretical shifts and the required numerical ones to be negligibly small (see a comparison along the two last columns of Table 1 given in ref 3a).

II.5. Bare and Dressed Diabatic Potentials To Study Topological Effects. Given the two adiabatic PESs $u_j(\theta,R|r)$. j = 1, 2, the corresponding Bare diabatic potentials $V_1(\theta,R|r)$, $V_2(\theta,R|r)$, and $V_{12}(\theta,R|r)$ are derived from the following set of equations:[19]

$$\begin{aligned} V_1(\theta,R|r) &= u_1(\theta,R|r)\cos^2\gamma(\theta,R|r) \\ &\quad + u_2(\theta,R|r)\sin^2\gamma(\theta,R|r) \\ V_2(\theta,R|r) &= u_1(\theta,R|r)\sin^2\gamma(\theta,R|r) \\ &\quad + u_2(\theta,R|r)\cos^2\gamma(\theta,R|r) \\ V_{12}(\theta,R|r) &= (1/2)\{u_2(\theta,R|r) - u_1(\theta,R|r)\}\sin(2\gamma(\theta,R|r)) \end{aligned} \tag{17}$$

where the $\gamma(\theta,R|r)$ angles are extracted, by interpolation/extrapolation, from the values of $\gamma(\varphi,q|r)$ calculated for the required corresponding CS as described in sections II.1−II.4.

In general, Dressed potentials are formed by three-dimensional nuclear vib-rotational eigenfunctions[10,12] In the present treatment, like in our previous one,[1a] we carry out these studies for fixed r-values and consequently we employ two-dimensional *rotational* eigenfunctions.

The Dressed diabatic *potentials* are derived by the expression

$$\tilde{V}_j(R|r) = \langle\xi_{0j}(\theta|R,r)|V_j(\theta|R,r)|\xi_{0j}(\theta|R,r)\rangle \tag{18a}$$

and the corresponding Dressed diabatic *coupling* term is given by

$$\tilde{V}_{12}(R|r) = \langle\xi_{01}(\theta|R,r)|V_{12}(\theta|R,r)|\xi_{02}(\theta|R,r)\rangle \tag{18b}$$

where $\xi_{0j}(\theta|R,r)$, j = 1, 2, are the lowest *rotational* eigenfunctions of the two *relevant* diabatic potentials, $V_j(\theta|R,r)$, j = 1, 2 (see Appendix I).

Next is formed the corresponding 2 × 2 Dressed *diabatic* potential matrix

$$\mathbf{V}(R|r) = \begin{pmatrix} \tilde{V}_1(R|r) & \tilde{V}_{12}(R|r) \\ \tilde{V}_{12}(R|r) & \tilde{V}_2(R|r) \end{pmatrix} \tag{19}$$

This matrix is then diagonalized to calculate the lower eigenvalue, $u_d(R|r)$, which is defined as the lowest adiabatic-via-Dressed-diabatic potentials.

In the numerical study we concentrate on the two kinds of *Dressed* adiabatic potentials: the just mentioned $u_d(R|r)$ and $u_a(R|r)$, which is the ordinary lowest Dressed adiabatic potential given in the form

$$u_a(R|r) = \langle\zeta_{01}(\theta|R,r)|u_1(\theta|R,r)|\zeta_{01}(\theta|R,r)\rangle \tag{20}$$

where $u_1(\theta|R,r)$ is the *Bare* adiabatic potential and $\zeta_{01}(\theta|R,r)$ is the corresponding lowest *rotational* eigenfunction of $u_1(\theta|R,r)$ (more about this calculation is given in Appendix I)

III. NUMERICAL RESULTS

III.1. Introductory Comments. As mentioned earlier, we apply the numerical treatment to the H_2 + F system for the situation described in section II.2.

The quasi-JT-NACTs are generated by MOLPRO[20] (see Appendix II for details). In this system the quasi-JT *ci* and the corresponding NACT are formed by a Σ state, assigned as 2A′ and one of the two Π states (with the same symmetry). The RT *degeneracy* is formed by the corresponding two Π states, designated as 1A′ and 1A″ which, as usual, are located along the (collinear) HHF axis. The corresponding RT-NACTs, which are required for the present study, are not calculated but derived theoretically as described in section II.4.1 and later in section II.4.3.

In what follows are discussed ADT angles, PESs, and the corresponding Dressed (and Bare) potential energy curves relevant for the present study. These are based on the SW pure adiabatic PESs[2a] calculated by employing the internally contracted multiconfiguration interaction (MRCI) method and the Davidson correction[21] using the MOLPRO program.[20] More details are given in ref 1.

III.2. Results. *III.2.1. Adiabatic-to-Diabatic Transformation Angles.* In Figure 2 are presented the (vertical) shifted (1,2) ADT angles, $\gamma_{12}(\varphi,q|r)$, as calculated according to the recipe in eqs 10−12. Some of the NACTS used in these calculations are presented in our recent articles.

In each of the three-panel figures are presented results along several circles (9 in panel a and 5 in panels b and c) with radii in the range $0.4 < q < 5.0$ au for the corresponding three r-values, namely, r = 1.4, 1.6, and 1.8 au. The important feature to notice is that the geometrical phase, $\alpha(q|r)$ (see eq 13), for most curves, is practically π (thus they all surround one (1,2) *ci*). There are two exceptions, namely the curves formed in cases {r = 1.4, q = 0.4} au and {r = 1.6, q = 0.4} au. Here we have $\alpha(q|r) = 0$, which implies that the relevant curves do not surround the (1,2)*ci*.

The second feature to notice is that except for the two lowest q-curves (namely, q = 0.4, 1.0 au) all other curves are shifted downward (at $\varphi = \pi$) to a varying degree. At this stage we emphasize again that the downward shifts for all cases are calculated according to eqs 10−12, where η is given by eq 16. In other words *no fitting* was exerted to achieve the required quantization!

The third feature to notice is that the φ dependence of the various curves become similar (in other words, the curves converge to each other) as the radius, q, of the circles increases. This phenomenon is general and nice to have (but not obvious) is enhanced along the interval: $\pi/2 < \varphi < 3\pi/4$.

III.2.2. Adiabatic and Diabatic Equi-potential Lines. In each of Figures 3−5 are compared the equi-potential lines for the two lower potentials, the adiabatic one, $u_1(R,\theta|r)$, and the diabatic one, $V_1(R,\theta|r)$ as calculated for r (=r_{HH}) = 1.4 au (Figure 3), 1.6 au (Figure 4), and 1.8 au (Figure 5). It is seen

dx.doi.org/10.1021/jp311014z | J. Phys. Chem. A 2013, 117, 8497−8505

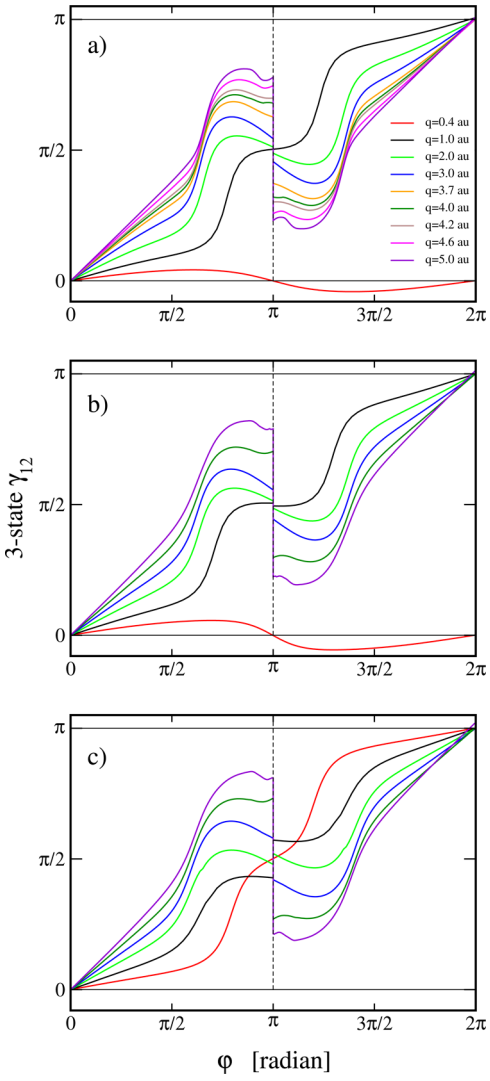

Figure 2. Tri-state ADT (mixing) angle, $\gamma_{12}(\varphi|q)$, for circular contours at $R = R_{ce} = 6$ au along the interval $0 \leq \varphi \leq 2\pi$ as calculated for the RT/JT topological effects employing eqs 11 and 12. Results are shown for $r = 1.4$ (a), $r = 1.6$ (b), and $r = 1.6$ (c).

that the two potentials differ significantly from each other although their main feature is similar—they both are characterized by a single potential barrier. This is in contrast to what we encountered in case the diabatic potentials were constructed employing *complementary* line integrals,[1a] which possess a typical *saddle* structure with the mini/max point located on the collinear axis (instead of a simple potential barrier).

III.2.3. Bare, Dressed Adiabatic, and Adiabatic-via-Dressed-Diabatic Potential Curves. In Figure 6 are given three panels, (a)−(c), presenting in each case three *R*-dependent, adiabatic, potential curves: (i) lower Dressed adiabatic potential, $u_a(R|r)$ (see eq 20); (ii) lower adiabatic via-Dressed-diabatic potential $u_d(R|r)$ (see eqs 17−19), and (iii) the corresponding *Bare* potential $u_1(\theta=0,R|r)$. It is important to emphasize that the values of all three potential curves in each panel are calculated by assuming the potential $u_1(\theta=0,R = 10|r)$, for all *r* values, is equal to zero.

The main feature to be seen is that in each case (panel) the three potential curves differ (sometimes quite significantly) from each other. This applies not only to the (collinear) Bare

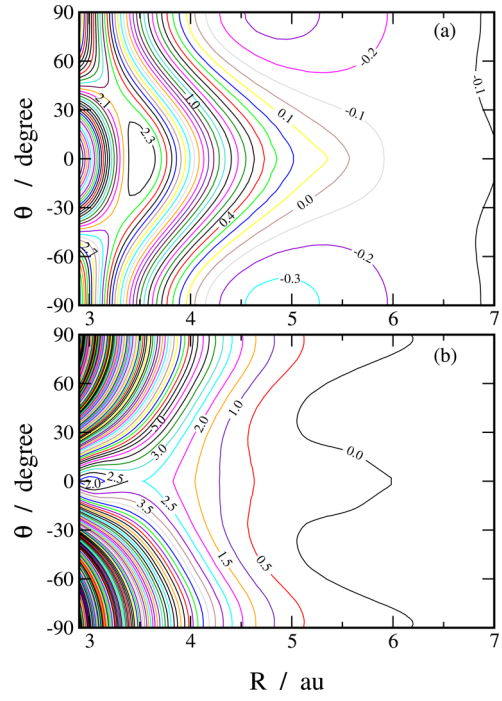

Figure 3. Equi-potential lines of the two potentials, namely, $u_1(R,\theta)$ (the lower adiabatic potential), presented in (a) and $V_1(R,\theta)$ (the lower diabatic potential), presented in (b) emphasizing the differences of their barrier structure (see text). The calculations were carried out for a plane formed by a fixed vibrational coordinate r ($=r_{HH}$) = 1.4 au.

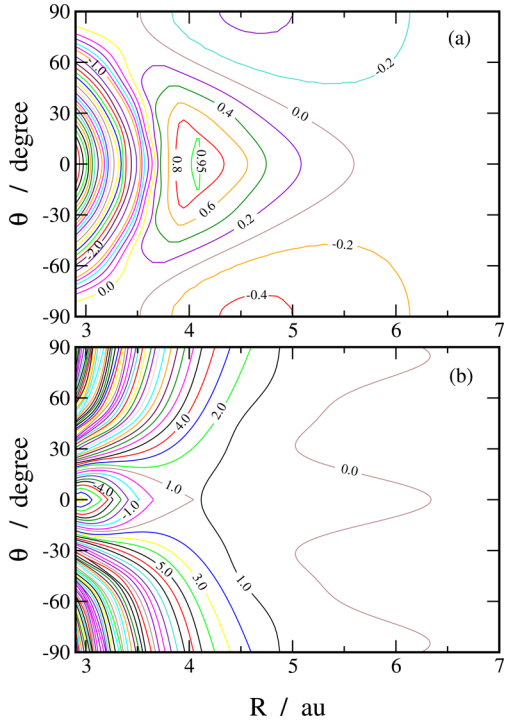

Figure 4. Same as in Figure 3 but for $r = 1.6$ au.

potential but also to the comparison between two types of Dressed adiabatic potentials. Two main features are noticed: (1) The smaller the interatomic distance, *r*, of H_2, the larger are the deviations between the two Dressed curves. (2) As *R* approaches the asymptotic region the two Dressed curves tend to overlap.

dx.doi.org/10.1021/jp311014z | J. Phys. Chem. A 2013, 117, 8497−8505

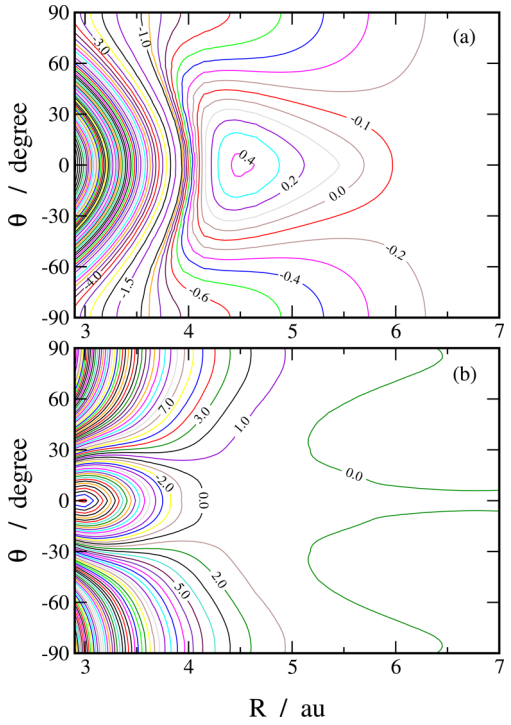

Figure 5. Same as in Figure 3 but for r = 1.8 au.

IV. DISCUSSION AND CONCLUSIONS

As was mentioned in the Introduction, our main goal in the present study is to reveal to what extent topological features of this system affect the lowest adiabatic PES. This is done by comparing two types of Dressed adiabatic potentials, namely, $u_a(R|r)$ and $u_d(R|r)$ as calculated for three different values of the H_2 inter atomic distance r (see section III.2.3 and Figure 6). A similar study was carried out, some time ago[1a] employing *complementary* line integrals, and in this case, a nice fit was obtained between the two types of Dressed potentials for all three vibronic cases. In the present case we face a somewhat different situation: in two cases (for r = 1.4, and r = 1.6 au) the two types of Dressed potentials differ significantly, whereas in the third case (r = 1.8 au) they deviate only slightly. Actually, the situation is more severe (as expressed just by the absolute numbers) because the large deviations take place in situations with higher probability. In other words, the system is more likely to be, during the (low energy) interaction, in the interval $1.3 < r < 1.5$ au rather than, for instance, at $r \sim 1.8$ au.

The main conclusion derived from our *previous* study[1a] was "The more interesting result of our study is, Mathematically speaking, that these two types of Dressed curves are not expected to overlap but if they do it will happen only under restrictive conditions. From the physical point of view this overlap indicates that the (1,2) *ci*, although it exists, does not affect significantly the lowest adiabatic potential. In other words dynamic calculations employing solely the lower adiabatic surface, as are done within the BO approximation, are expected to be only slightly affected by topological effects." (Examples for treatments within the BO approximation are given in refs 11, 12, and 22−26.)

The conclusion of the present study is different: Including the RT effect in the numerical treatment (in addition to the JT *ci*) yields Dressed potential curves that deviate significantly from each other, thus indicating that topological effects most likely influence processes taking place on the lower adiabatic PES. In other words, this study seems to imply that the BO

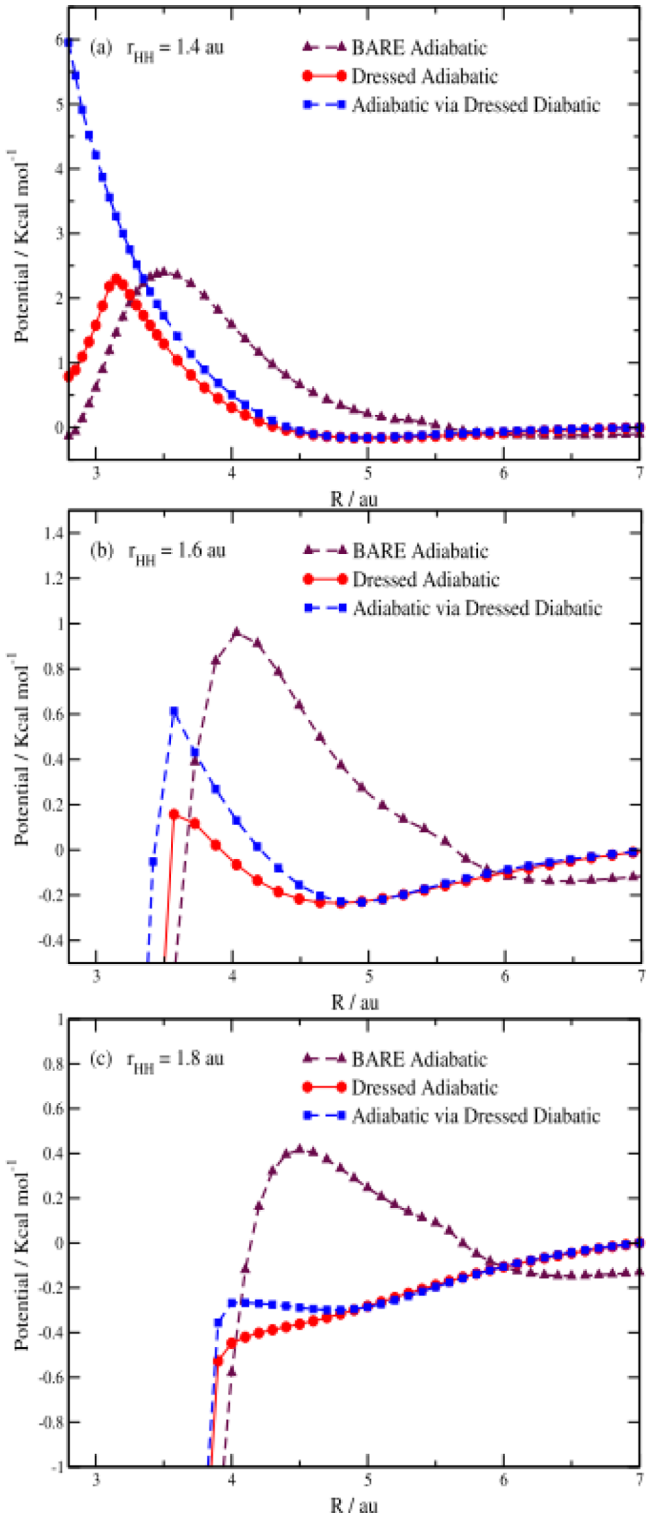

Figure 6. Potential curves calculated for fixed vibrational coordinates r ($=r_{HH}$). In each panel are presented three curves: (i) the bare adiabatic potential $u_1(R,\theta|r)$ calculated at θ = 0; (ii) the dressed adiabatic potential $u_a(R|r)$ (see eq 20); (iii) the adiabatic via dressed diabatic potential $u_d(R|r)$ obtained by diagonalizing the dressed *diabatic* potential matrix, $V(R|r)$ (see eqs 18 and eq 19). The results for r_{HH} = 1.4, 1.6, and 1.8 au are shown in (a), (b), and (c) respectively.

dx.doi.org/10.1021/jp311014z | J. Phys. Chem. A 2013, 117, 8497−8505

approximation may not be valid for the title system in general and in particular not for (ultra) *cold reactions*.

Finally the following comment: This conclusion reminds us of reactive scattering studies performed, a few years ago, for a two-arrangement model.[27] In these studies were coupled two (or more) adiabatic PESs via a JT-*ci* and in some cases quantum, state-selected, energy-dependent *reactive* transition probabilities were calculated. The results were then compared with corresponding *single-state* probabilities and were found to be similar.[27] The disappointing conclusion from this study, just like the one we have based on the *complementary* line integrals, is that JT-*cis* are barely capable of affecting magnitudes such as the *state-selected* probabilities. It could be interesting to see if including the RT effect in such a model will affect the corresponding probabilities as predicted in the present study.

APPENDIX I

Rotational Eigenfunctions and the Dressed Vib-Translational Potential

To derive the rotational eigenfunctions, we consider the following Hamiltonian, H_r:

$$H_r(\theta|R,r) = \frac{1}{2\mu r^2} j^2 + V(\theta|R,r) \tag{I.1}$$

where j^2 is an operator given in the form

$$j^2 = -\hbar^2 \frac{1}{\sin\theta}\frac{\partial}{\partial\theta}\sin\theta\frac{\partial}{\partial\theta} \tag{I.2}$$

Our aim is to solve the following eigenvalue problem:

$$(H_r(\theta|R,r) - \varepsilon(R,r))\xi(\theta|R,r) = 0 \tag{I.3}$$

and for this purpose we expand $\xi(\theta|R,r)$ in terms of Legendre polynomials, $P_j(\theta)$, namely

$$\xi_k(\theta|R,r) = \sum_{j=0} a_{kj}(R|r)\, P_j(\theta) \tag{I.4}$$

where $a_{kj}(R|r)$ are fixed coefficients to be determined next.

Substituting eqs I.1, I.2, and I.4 into eq I.3 and recalling that the Legendre polynomials are eigenfunctions of the operator j^2 (see eq I.2), we face the following eigenvalue problem:

$$\sum_{j'} (H_{rjj'}(R,r) - \delta_{jj'}\varepsilon_k(R|r))a_{kj'}(R|r) = 0 \tag{I.5}$$

where $H_{rjj'}$ are defined as

$$H_{rjj'}(R,r) = \langle P_j|V(\theta|R,r)|P_{j'}\rangle + \frac{\hbar^2}{2\mu_r r^2} j(j+1)\delta_{jj'} \tag{I.6}$$

Here

$$\langle P_j|V(\theta|R,r)|P_{j'}\rangle = \int_{-1}^{+1} \mathrm{d}\cos\theta P_j(\theta)\, V(\theta|R,r)\, P_{j'}(\theta) \tag{I.7}$$

where we recall

$$\int_{-1}^{+1} \mathrm{d}\cos\theta P_j(\theta)\, P_{j'}(\theta) = \delta_{jj'} \tag{I.8}$$

Solving the eigenvalue problem in eq I.5 yields the N eigenvectors, $\mathbf{a}_k(R,r)$ and the corresponding N eigenvalues ε_k; $k = 0, 1, ..., N-1$. In the present numerical study only the lowest eigenvalue ε_0 is required and the corresponding eigenfunction $\xi_0(\theta|R,r)$ is given in the form

$$\xi_0(\theta|R,r) = \sum_{j=0}^{N} a_{0j}(R,r)\, P_j(\theta) \tag{I.9}$$

Our study is concerned with the following vib-translational potentials $W_0(R|r)$ as calculated for a fixed value of r and a series of R values.

$$W_0(R|r) = \langle \xi_0(\theta|R,r)|V(\theta|R,r)|\xi_0(\theta|R,r)\rangle \tag{I.10}$$

APPENDIX II

Numerical Quantum Chemistry

The calculation of the NACTs (along chosen circles) was carried out at the state-average CASSCF level using the MOLPRO program.[20] Within this calculation we used all seven valence electrons distributed on eight (8) orbitals. Six electronic states, including the two/three studied states, were computed by this method applying equal weights. The active space is made up of the $3\sigma-6\sigma$ orbitals, 1π valence orbital and one additional set of correlating π-orbitals. Care has been taken to avoid the swap of 2σ and 3σ orbitals during the optimization of the orbitals at the CASSCF level.[2a,20] The basis sets employed are (a) for the hydrogens we employed s functions from the cc-pV5Z set and p and d functions from the cc-pVQZ set augmented with diffuse s and p functions and (b) for the fluorine we applied s and p functions from the cc-pV5Z set and d and f functions from cc-pVQZ set augmented with diffuse s, p, d and f functions;

Adiabatic potential energy surfaces (PESs) of the two lowest adiabatic states, 1A′ and 2A′ (which correspond to a Π state and a Σ state), have been generated at MRCI level added with Davidson correction[21] using MOLPRO program[20] As before, the active space has been composed of the $3\sigma-6\sigma$ orbitals, 1π valence orbitals, and one additional set of correlating 2π orbitals. Before the MRCI calculation was performed, at the state-average CASSCF level, the three lowest electronic states, including the two studied ones, were computed with equal weights. The rest is as before.

AUTHOR INFORMATION

Corresponding Author

*E-mail: michaelb@fh.huji.ac.il.

Notes

The authors declare no competing financial interest.

ACKNOWLEDGMENTS

This work was partially supported by the Romanian National Authority for Scientific Research (ANCS) through the PN-II-RU-TE-2011-3-0124 Research Project. A.B. gratefully acknowledges the Data Center of NIRDIMT Cluj-Napoca for providing the computational infrastructure and the technical assistance. A.V. acknowledges the computational resources provided by the John-von-Neumann Institute, Research Centre Juelich (Project ID ehu01) and the OTKA (NN103251). The publication was supported by the TÁMOP-4.2.2.C-11/1/KONV-2012-0001 project. The project has been supported by the European Union, cofinanced by the European Social Fund. M.B. thanks Professor R. Englman, from the Soreq Nuclear Research Center, Yavne, Israel, for a discussion during which the possibility of the formation of a third *effect*, namely, the RT/JT effect, was considered for the first time.

REFERENCES

(1) (a) Das, A.; Sahoo, T.; Mukhopadhyay, D.; Adhikari, S.; Baer, M. *J. Chem. Phys.* **2012**, *136*, 054104-1−054104-6. (b) Das, A.; Mukhopadhyay, D.; Adhikari, S.; Baer, M. *Chem. Phys. Lett.* **2011**, *517*, 92−97. (c) Das, A.; Mukhopadhyay, D.; Adhikari, S.; Baer, M. *Eur. Phys. J. D* **2011**, *65*, 373−381.

(2) (a) Stark, K.; Werner, H.-J. *J. Chem. Phys.* **1996**, *104*, 6515−6530. (b) Alexander, M. H.; Werner, H. J.; Manolopoulos, D. E. *J. Chem. Phys.* **1998**, *109*, 5710−5713. (c) Alexander, M. H.; Manolopoulos, D. E.; Werner, H.-J. *J. Chem. Phys.* **2000**, *113*, 11084-1−11084-17.

(3) (a) Das, A.; Mukhopadhyay, D.; Adhikari, S.; Baer, M. *Int. J. Quantum Chem.* **2012**, *112*, 2561−2570. (b) Csehi, A.; Bende, A.; Halász, G. J.; Vibók, Á.; Das, A.; Mukhopadhyay, D.; Baer, M. *J. Chem. Phys.* **2013**, *138*, 024113-1−024113-11.

(4) Baer, M. *Chem. Phys. Lett.* **1975**, *35*, 112−118. Yarkony, D. R. In Domcke, W., Yarkony, D. R., Köppel, H., Eds. *Conical Intersections: Electronic Structure, Dynamics and Spectroscopy*; World Science: Singapore, 2004; pp 41−127. Ryb, I.; Baer, R. *J. Chem. Phys.* **2004**, *121*, 10370-6−10370-6. Baer, M.; Vertesi, T.; Halász, G. J.; Vibók, Á.; Suhai, S. *Farad. Discuss.* **2004**, *127*, 337−353. Sarkar, B.; Adhikari, S. *J. Phys. Chem. A* **2008**, *112*, 9868−9885. Kaczmarski, M. S.; Ma, Y.; Rohlfing, M. *Phys. Rev. B* **2010**, *81*, 115433-1−115433-9. Al-Jabour, S.; Baer, M.; Deeb, O.; Liebscher, M.; Manz, J.; Xu, X.; Zilberg, S. *J. Phys. Chem. A* **2010**, *114*, 2991−3010. Sirjoosingh, A.; Hammes-Schiffer, S. *J. Phys. Chem. A* **2011**, *115*, 2367−2377. Labuda, M.; Gonzalez-Vazquez, J.; Fernando, M.; Gonzalez, L. *Chem. Phys.* **2012**, *400*, 165−170.

(5) Baer, M. *Beyond Born Oppenheimer; Electronic non-Adiabatic coupling Terms and Conical Intersections*; Wiley & Sons Inc.: Hoboken, NJ, 2006; section 1.3, pp 11−22.

(6) Halász, G. J.; Vibók, Á.; Baer, R.; Baer, M. *J. Chem. Phys.* **2006**, *125*, 094102-1−094102-9. Halász, G. J.; Vibók, Á.; Hoffman, D. K.; Kouri, D. J.; Baer, M. *J. Chem. Phys.* **2007**, *126*, 154309-1−154309-13.

(7) (a) Das, A.; Mukhopadhyay, D.; Adhikari, S.; Baer, M. *J. Chem. Phys.* **2010**, *133*, 084107-1−084107-11. (b) Das, A.; Mukhopadhyay, D. *J. Phys. Chem. A* **2012**, *116*, 1774−1785.

(8) Top, Z. H.; Baer, M. *Chem. Phys.* **1977**, *25*, 1−18. Baer, M.; Niedner, G.; Toennies, J. P. *J. Chem. Phys.* **1989**, *91*, 4169−4182. Liao, C. L.; Xu, R.; Flesh, G. D.; Baer, M.; Ng, C. Y. *J. Chem. Phys.* **1990**, *93*, 4818−4831.

(9) (a) Levy, C.; Halász, G. J.; Vibók, Á.; Bar, I.; Zeiri, I. Y.; Kosloff, R.; Baer, M. *J. Chem. Phys.* **2008**, *128*, 244302−1−244302−6;(b) Levy, C.; Halász, G. J.; Vibók, Á.; Bar, I.; Zeiri, I. Y.; Kosloff, R.; Baer, M. *Int. J. Quantum Chem.* **2009**, *109*, 2482−2489.

(10) (a) Lipoff, S. H.; Herschbach, D. *Mol. Phys.* **2010**, *108*, 1133−1143. See also: Herschbach, D. *Faraday Discuss.* **2009**, *142*, 9−23.

(11) Bodo, E.; Gianturco, F. A.; Dalgarno, A. *J. Chem. Phys.* **2002**, *116*, 9222−9227. Balakrishnan, N.; Dalgarno, A. *J. Phys. Chem. A* **2003**, *107*, 7101−7105. Krems, R. V. *Int. Rev. Phys. Chem.* **2005**, *24*, 99−118. Weck, P. F.; Balakrishnan, N. *Int. Rev. Phys. Chem.* **2006**, *25*, 283−311. Bovino, S.; Taccomi, M.; Gianturco, F. A. *J. Phys. Chem. A* **2011**, *115*, 8197−8203.

(12) Rosenman, E.; Hochman-Kowal, Z.; Persky, A.; Baer, M. *Chem. Phys. Lett.* **1996**, *257*, 421−428.

(13) Born, M.; Oppenheimer, J. R. *Ann. Phys.(Leipzig)* **1927**, *84*, 457−488. Born, M.; Huang, K., *Dynamical theory of Crystal Lattices*; Oxford University: New York, 1954; Chapter IV.

(14) Reference 5, section 5.1 (pp 105−108).

(15) Baer, M. *J. Phys. Chem. A* **2000**, *104*, 3181−3184. Baer, M.; Lin, S. H.; Alijah, A.; Adhikari, S.; Billing, G. D. *Phys. Rev. A* **2000**, *62*, 032506-1−032506-8. Reference 5, section 2.1.3.3 (pp 34−38).

(16) (a) Top, Z. H.; Baer, M. *J. Chem. Phys.* **1977**, *66*, 1363−1371. (b) Alijah, A.; Baer, M. *J. Phys. Chem. A* **2000**, *104*, 389−396. (c) Reference 5, section 5.5.3 (pp 127−130). (d) Sarkar, B.; Adhikari, S. *J. Phys. Chem. A* **2008**, *112*, 9868−9885.

(17) Vertesi, T.; Bene, E.; Vibók, Á.; Halász, G. J.; Baer, M. *J. Phys. Chem. A* **2005**, *109*, 3476−3484.

(18) (a) Top, Z. H.; Baer, M. *Chem. Phys.* **1977**, *25*, 1−18 (see Appendix A). (b) Baer, M.; Mebel, A. M.; Billing, G. D. *Int. J. Quantum Chem.* **2002**, *90*, 1577−1585.

(19) Baer, M. *Adv. Chem. Phys.* **1982**, *49*, 191−322 (see p 283). Reference 5, section 3.1.1.3 (pp 61−62).

(20) MOLPRO is a package of ab initio programs written by H. J. Werner and P. J. Knowles, with contributions from J. Almlöf et al.

(21) Langhoff, S. R.; Davidson., E. R. *Int. J. Quantum Chem.* **1974**, *8*, 61−72.

(22) Baer, M.; Faubel, M.; Martinez-Haya, B.; Rusin, L. Y.; Tapp, U.; Toennies, J. P.; Stark, K.; Werner, H.-J *J. Chem. Phys.* **1996**, *104*, 2743−2745. Baer, M.; Faubel, M.; Martinez-Haya, B.; Rusin, L. Y.; Tapp, U.; Toennies, J. P. *J. Chem. Phys.* **1998**, *108*, 9694−9710.

(23) Manolopoulos, D. E. *Faraday Trans., Chem. Soc.* **1997**, *93*, 673−683.

(24) Zhang, D. H.; Lee, S.-Y.; Baer, M. *J. Chem. Phys.* **2000**, *112*, 9802−9809.

(25) Aoiz, F. J.; Banares, L.; Castillo, F. *J. Chem. Phys.* **1999**, *111*, 4013−4024. Martinez-Haya, B.; Aoiz, F. J.; Banares, L.; Honvault, P.; Launay, J. M. *Phys. Chem. Chem. Phys.* **1999**, *1*, 3415−3427.

(26) Aquilanti, J. M.; Cavalli, S.; De Fazio, D.; Volpi, A.; Aguilar, A.; Maria Lucas, J. *Chem. Phys.* **2005**, *308*, 237−253.

(27) (a) Baer, R.; Charutz, D. M.; Kosloff, R.; Baer, M. *J. Chem. Phys.* **1996**, *105*, 9141−9152. (b) Charutz, D. M.; Baer, R.; Baer, M. *Chem. Phys. Lett.* **1997**, *265*, 629−637. (c) Adhikari, S.; Billing, G. D. *J. Chem. Phys.* **1999**, *111*, 40−47. (d) Baer, M.; Lin, S. H.; Alijah, A.; Adhikari, S.; Billing, G. D. *Phys. Rev. A* **2000**, *62*, 032506-1−032506-1. (e) Puzari, P.; Sarkar, B.; Adhikari, S. *J. Chem. Phys.* **2004**, *121*, 707−721. (f) Sarkar, B.; Varandas, A. J. C. *Chem. Phys.* **2011**, *389*, 81−87.